Supplementary Information

- Supplementary Figures 1-8
- Supplementary Figures legends
- Supplementary Materials and Methods
- Supplementary Table 1 (Primer information)
- Supplementary Table 2 (Antibody information)
- Supplementary Table 3 (Gene list of DEGs in excel file)
- Supplementary References

Sup. Figure 1

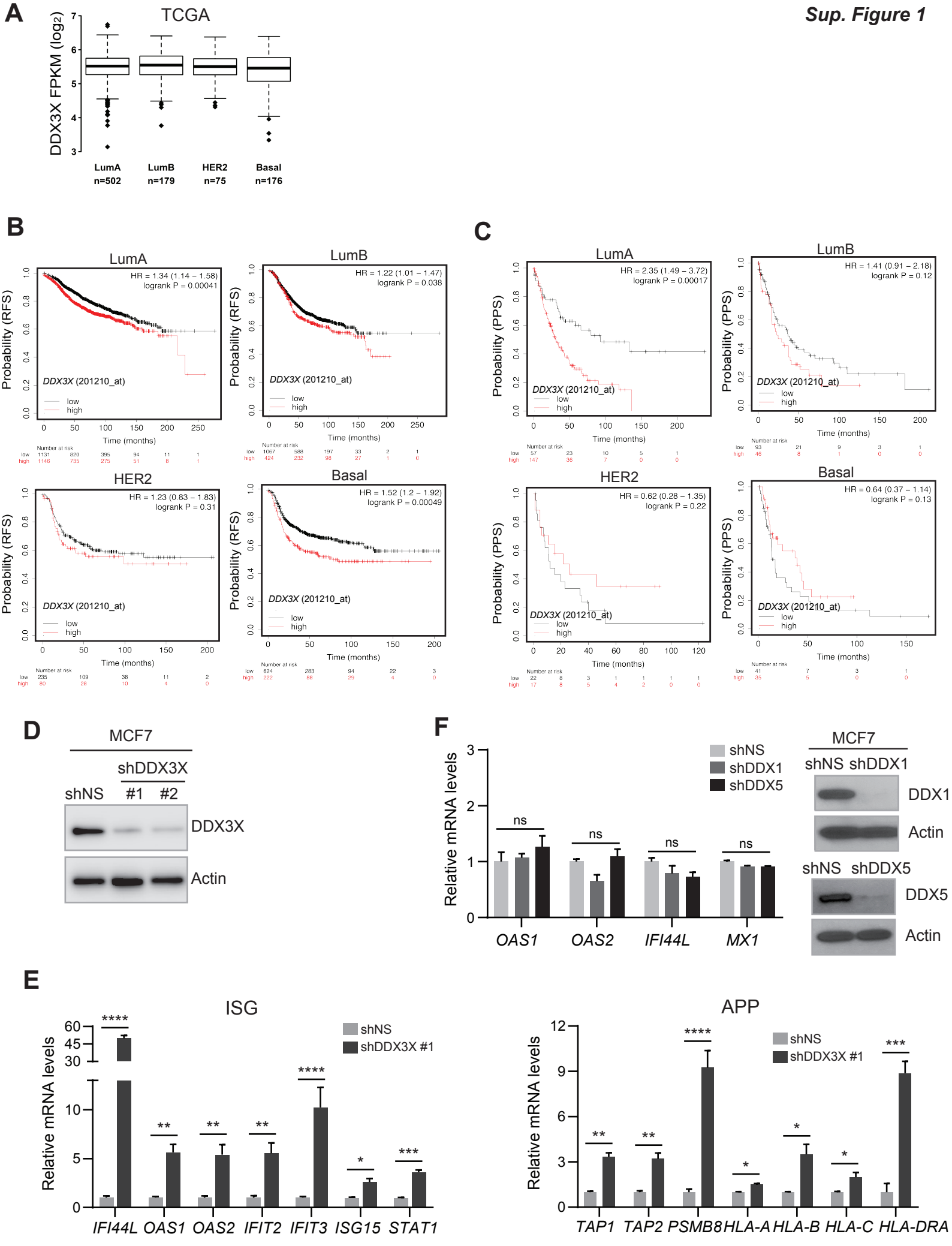
A
TCGA
DDX3X FPKM (log2)
LumA n=502
LumB n=179
HER2 n=75
Basal n=176
B
LumA
HR = 1.34 (1.14 – 1.58)
logrank P = 0.00041
LumB
HR = 1.22 (1.01 – 1.47)
logrank P = 0.038
HER2
HR = 1.23 (0.83 – 1.83)
logrank P = 0.31
Basal
HR = 1.52 (1.2 – 1.92)
logrank P = 0.00049
Probability (RFS)
DDX3X (201210_at)
low
high
Time (months)
Number at risk
C
LumA
HR = 2.35 (1.49 – 3.72)
logrank P = 0.00017
LumB
HR = 1.41 (0.91 – 2.18)
logrank P = 0.12
HER2
HR = 0.62 (0.28 – 1.35)
logrank P = 0.22
Basal
HR = 0.64 (0.37 – 1.14)
logrank P = 0.13
Probability (PPS)
D
MCF7
shDDX3X
shNS
#1
#2
DDX3X
Actin
F
MCF7
shNS
shDDX1
shDDX5
Relative mRNA levels
ns
OAS1
OAS2
IFI44L
MX1
DDX1
Actin
DDX5
E
ISG
APP
shNS
shDDX3X #1
Relative mRNA levels
IFI44L
OAS1
OAS2
IFIT2
IFIT3
ISG15
STAT1
TAP1
TAP2
PSMB8
HLA-A
HLA-B
HLA-C
HLA-DRA

Supplementary Figure 1. High expression of DDX3X correlates with worse prognosis and knockdown of DDX3X upregulates genes in the antiviral innate immune response.

A. The level of *DDX3X* transcript in luminal A, luminal B, HER2+, and basal-like breast cancer patients (TCGA), Fragments per Kilobase of transcript per Million mapped reads (FPKM).

B. Relapse-free survival (RFS) analysis of DDX3X in luminal A, luminal B, HER2+, and basal-like breast cancer patients.

C. Post-progression survival (PPS) analysis of DDX3X in luminal A, luminal B, HER2+, and basal-like breast cancer patients.

D. Western blot analysis of DDX3X knockdown by two different shRNAs (shDDX3X_#1, #2) in MCF7 cells. shNS, non-specific shRNA.

E. qRT-PCR of ISGs and APP genes in DDX3X-control or -KD (shDDX3X_#1) MCF7 cells.

F. qRT-PCR of ISGs in DDX1-KD or DDX5-KD MCF7 cells.

Data are shown as mean ± SEM of three independent experiments. Statistical significance was calculated using unpaired t-tests. *$p < 0.05$; **$p< 0.01$; ***$p < 0.001$; ****$p < 0.0001$; ns, not significant.

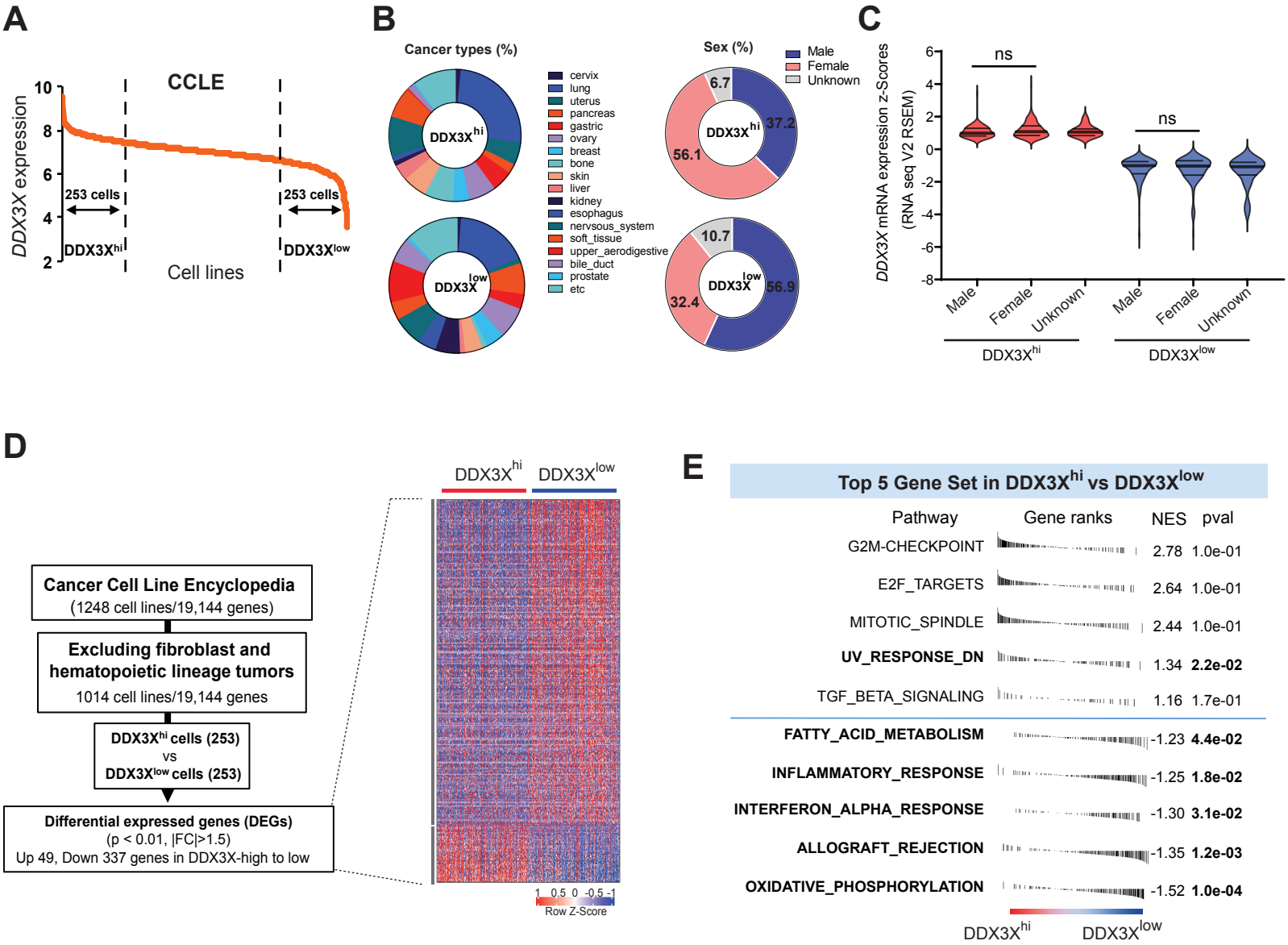

6-gene MHC class I

HLA-A	*HLA-B*	*HLA-C*	*HLA-E*	*HLA-F*
HLA-G				

13-gene MHC class II

HLA-DMA	*HLA-DMB*	*HLA-DOA*	*HLA-DOB*	*HLA-DPA1*
HLA-DPB1	*HLA-DQA1*	*HLA-DQA2*	*HLA-DQB1*	*HLA-DQB2*
HLA-DRA	*HLA-DRB1*	*HLA-DRB5*		

Supplementary Figure 2. Low DDX3X expression is related to chronic activation of the innate antiviral immune response in various cancer cell lines.

A. $DDX3X^{hi}$ and $DDX3X^{low}$ cancer cells in CCLE.

B. Cancer type and sex of cancer cells in $DDX3X^{hi}$ and $DDX3X^{low}$ group.

C. *DDX3X* transcript level in each group defined by sex in $DDX3X^{hi}$ and $DDX3X^{low}$ group.

D. Flowchart leading to the identification of differentially expressed genes (DEGs) between $DDX3X^{hi}$ and $DDX3X^{low}$ cells.

E. Gene set enrichment analysis (GSEA) plots with the Molecular Signatures Database (MSigDB). (Significantly enriched gene sets are highlighted in bold)

F. Violin plots showing transcript levels of MHC I, MHC II, IFNs, interleukin 6 genes in $DDX3X^{hi}$ and $DDX3X^{low}$ group. MHC genes used in calculation of MHC core score (below).

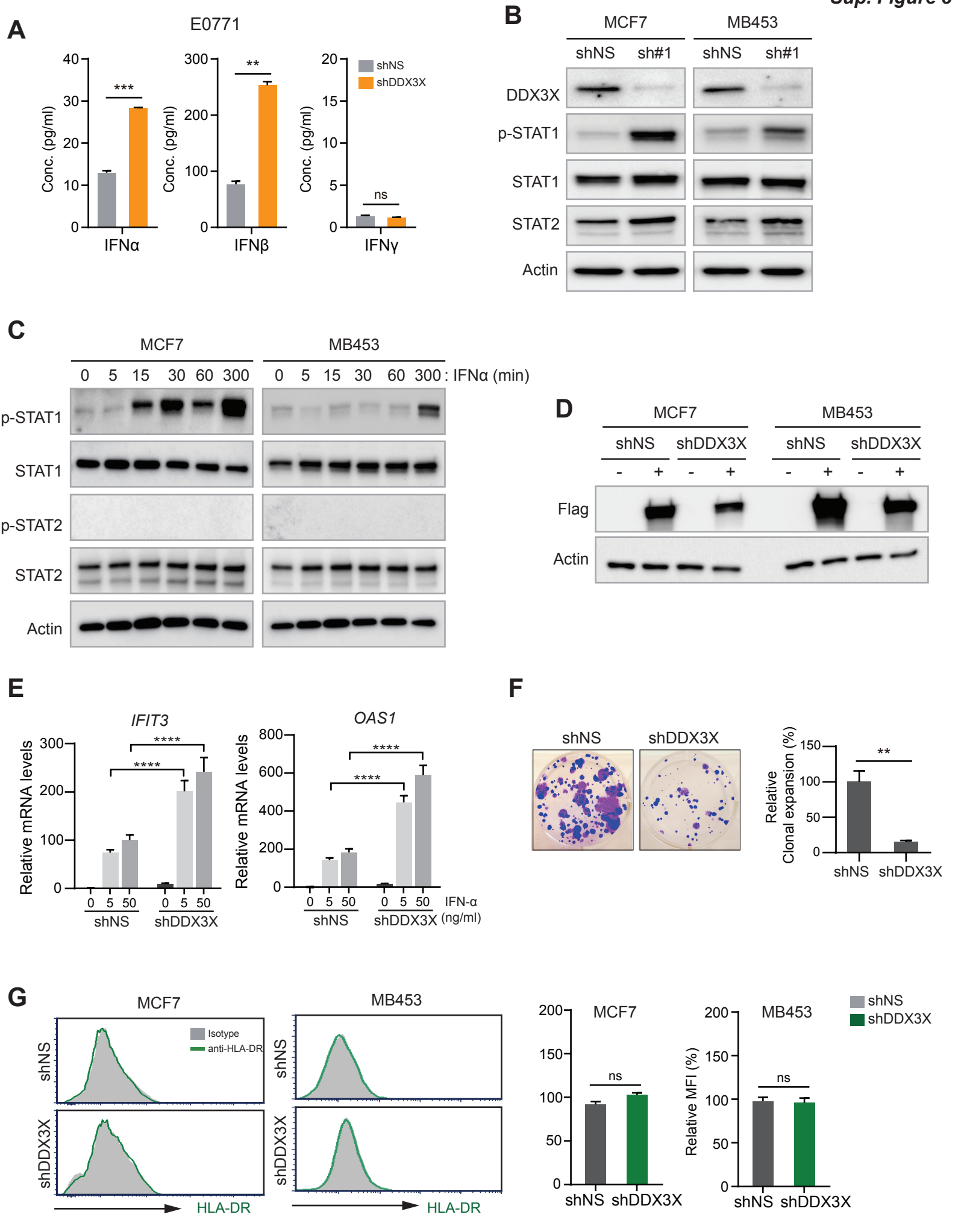
A
E0771
Conc. (pg/ml)
IFNα
IFNβ
IFNγ
shNS
shDDX3X
***
**
ns
B
MCF7
MB453
shNS
sh#1
DDX3X
p-STAT1
STAT1
STAT2
Actin
C
MCF7
MB453
0 5 15 30 60 300 : IFNα (min)
p-STAT1
STAT1
p-STAT2
STAT2
Actin
D
MCF7
MB453
shNS
shDDX3X
Flag
Actin
E
IFIT3
OAS1
Relative mRNA levels
IFN-α (ng/ml)
shNS
shDDX3X
****
F
shNS
shDDX3X
Relative Clonal expansion (%)
G
MCF7
MB453
Isotype
anti-HLA-DR
HLA-DR
Relative MFI (%)
ns

Supplementary Figure 3. Loss of DDX3X induces type I IFN production, STAT1 activation, and antigen processing and presentation.

A. ELISA of IFN-α, -β, and -γ in the culture supernatants from DDX3X-control or -KD E0771 cells.

B. Western blot analysis of phospho-STAT1, STAT1, and STAT2 in the DDX3X-control or - KD MCF7 cells using shDDX3X_#1.

C. Western blot analysis of phospho-STAT1, STAT1, phospho-STAT2, and STAT2 in MCF7 or MDA-MB-453 cells with 5 ng/ml of IFN-α treatment.

D. Western blot validation of DDX3X overexpression by transfecting flag-tagged DDX3X overexpression vector.

E. qRT-PCR of *IFIT3* and *OAS1* in DDX3X-control or -KD MCF7 cells after IFN-α treatment for 5 hours.

F. Colony formation assay in DDX3X-control or -KD MCF7 cells (left). Intensity of crystal violet stained was measured by Image J (right).

G. Representative flow histograms and a bar graph of MHC class II (HLA-DR) in the DDX3X-KD MCF7 or DDX3X-KD MDA-MB-453 cells.

Data are shown as mean ± SEM of three independent experiments. Statistical significance was calculated using unpaired t-tests. $^{**}p < 0.01$; $^{***}p < 0.001$; $^{****}p < 0.0001$; ns, not significant.

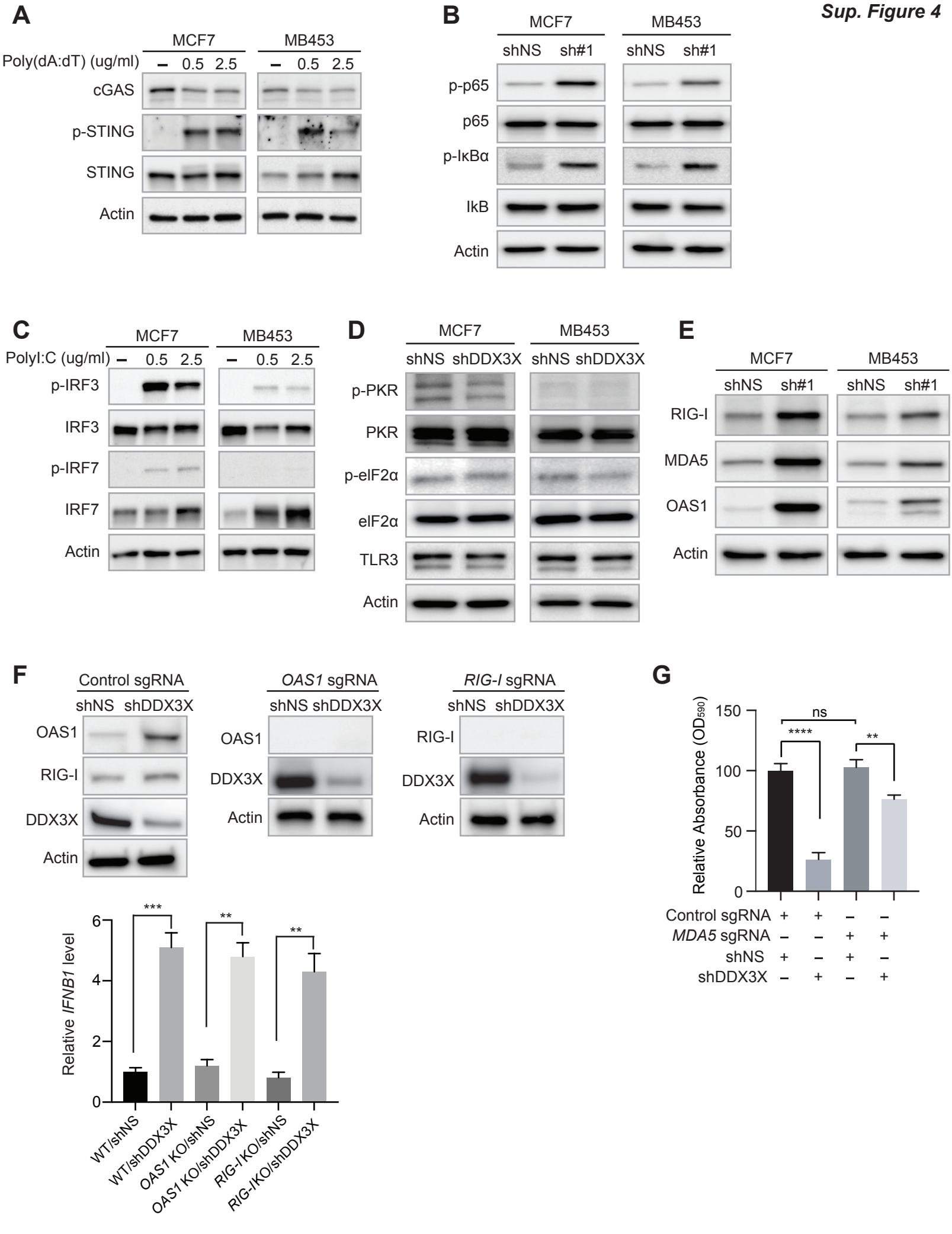
A
MCF7
MB453
Poly(dA:dT) (ug/ml)
–
0.5
2.5
cGAS
p-STING
STING
Actin
B
MCF7
MB453
shNS
sh#1
p-p65
p65
p-IκBα
IkB
Actin
C
MCF7
MB453
PolyI:C (ug/ml)
p-IRF3
IRF3
p-IRF7
IRF7
Actin
D
MCF7
MB453
shNS
shDDX3X
p-PKR
PKR
p-eIF2α
eIF2α
TLR3
Actin
E
MCF7
MB453
shNS
sh#1
RIG-I
MDA5
OAS1
Actin
F
Control sgRNA
OAS1 sgRNA
RIG-I sgRNA
shNS
shDDX3X
OAS1
RIG-I
DDX3X
Actin
Relative IFNB1 level
***
**
**
WT/shNS
WT/shDDX3X
OAS1 KO/shNS
OAS1 KO/shDDX3X
RIG-I KO/shNS
RIG-I KO/shDDX3X
G
Relative Absorbance (OD590)
ns
****
**
Control sgRNA
MDA5 sgRNA
shNS
shDDX3X

Supplementary Figure 4. dsRNA sensing MDA5-NFκB signaling axis leads to type I IFN production in DDX3X-KD breast cancer cells.

A. Western blot analysis of STING, phosphorylation of STING, and cGAS in MCF7 and MDA-MB-453 cells treated with poly(dA:dT) for 24 hours.

B. Western blot analysis of phosphorylation of NFκB p65 and IκBα in DDX3X-control or -KD MCF7 or MDA-MB-453 cells.

C. Western blot analysis of phosphorylation of TBK1, IRF3, and IRF7 in MCF7 and MDA-MB-453 cells treated with poly I:C for 24 hours.

D. Western blot analysis of phospho-PKR, PKR, phospho-eIF2α, eIF2α, and TLR3 in DDX3X-control or -KD MCF7 or MDA-MB-453 cells.

E. Western blot analysis of RIG-I, OAS1, and MDA5 in DDX3X-control or -KD MCF7 or MDA-MB-453 cells.

F. Western blot validation of CRISPR/Cas9-mediated *OAS1* or *RIG-I* knockout (KO). qRT-PCR of *IFNB1* in *OAS1* or *RIG-I* -wildtype (WT) or -KO MCF7 cells followed by DDX3X-control or -KD.

G. Colony formation of *MDA5* -WT or -KO MCF7 cells 7 days after DDX3X KD. Crystal violet absorbance (OD 590) of attached cells was quantified, and *MDA5* WT/shNS groups were normalized to 100%.

Data are shown as mean ± SEM of three independent experiments. Statistical significance was calculated using unpaired t-tests. *$p < 0.05$; **$p < 0.01$; ***$p < 0.001$; ****$p < 0.0001$; ns, not significant.

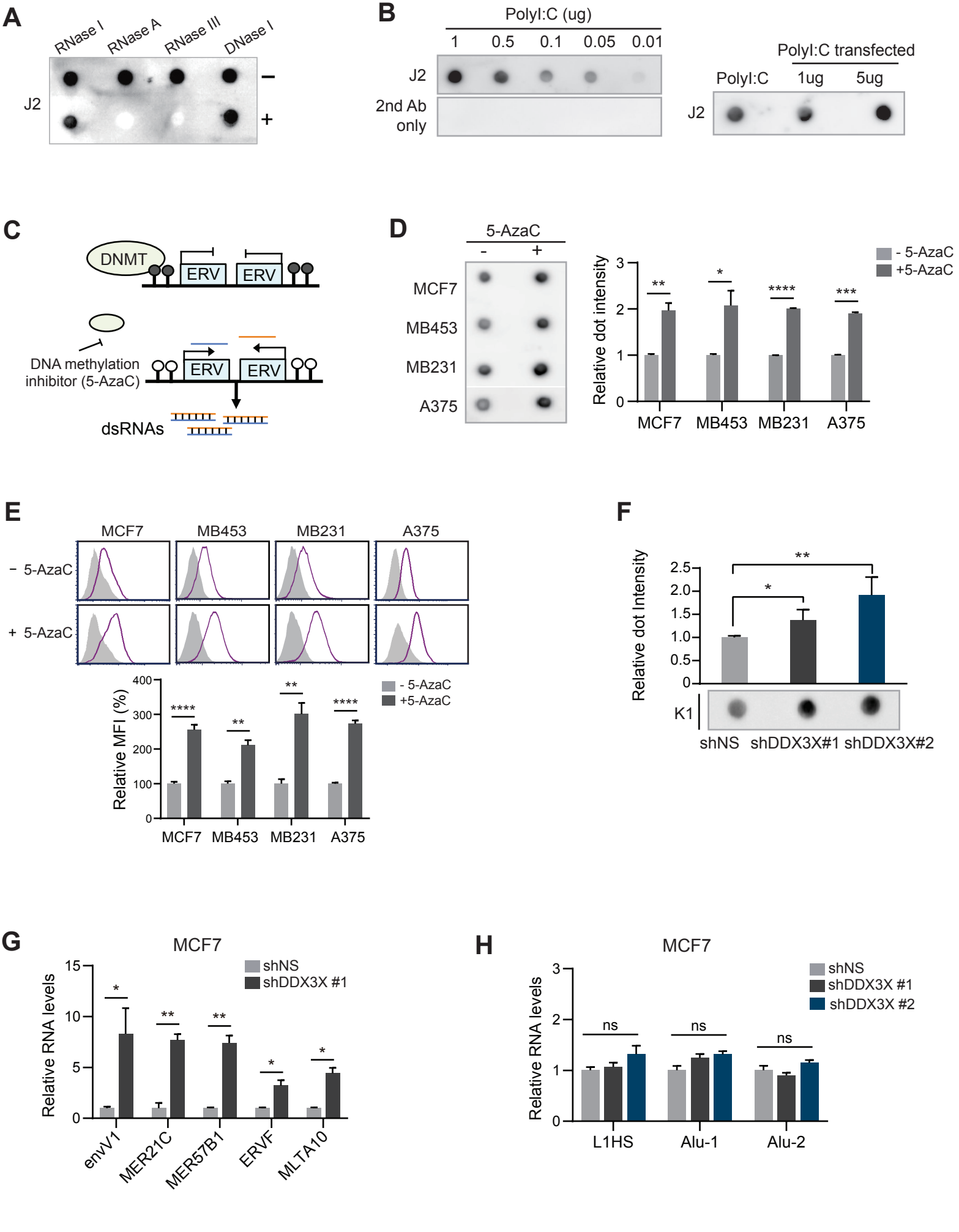
A
RNase I
RNase A
RNase III
DNase I
J2
−
+
B
PolyI:C (ug)
1
0.5
0.1
0.05
0.01
J2
2nd Ab only
PolyI:C transfected
PolyI:C
1ug
5ug
J2
C
DNMT
ERV
ERV
DNA methylation inhibitor (5-AzaC)
ERV
ERV
dsRNAs
D
5-AzaC
-
+
MCF7
MB453
MB231
A375
Relative dot intensity
- 5-AzaC
+5-AzaC
MCF7
MB453
MB231
A375
E
MCF7
MB453
MB231
A375
− 5-AzaC
+ 5-AzaC
Relative MFI (%)
- 5-AzaC
+5-AzaC
MCF7
MB453
MB231
A375
F
Relative dot Intensity
K1
shNS
shDDX3X#1
shDDX3X#2
G
MCF7
shNS
shDDX3X #1
Relative RNA levels
envV1
MER21C
MER57B1
ERVF
MLTA10
H
MCF7
shNS
shDDX3X #1
shDDX3X #2
Relative RNA levels
ns
L1HS
Alu-1
Alu-2

Supplementary Figure 5. Knockdown of DDX3X triggers the cytoplasmic accumulation of endogenous dsRNAs.

A. Dot blot analysis using J2 antibody in RNA extracted from MCF7 cells treated with RNases and DNase.

B. Dot blot analysis with poly I:C (left) or RNA extracts from poly I:C transfected cells (right).

C. Schema of DNA methyltransferase inhibitor (5-AzaC) action on dsRNA formation of ERVs.

D. and E. Increased endogenous dsRNA levels were analyzed by dot blot (D) and flow cytometry (E) after 5-AzaC treatment in each cell. Bar graphs represent relative dot intensity (D) and relative MFI (E).

F. Dot blot analysis using K1 antibody with total RNAs extracted from DDX3X-control or -KD MCF7 cells. Graph shows relative dot intensity.

G. qRT-PCR of ERV genes in DDX3X-control or -KD MCF7 cells.

H. qRT-PCR of L1HS and Alu in DDX3X-control or -KD MCF7 cells.

Data are shown as mean ± SEM of three independent experiments. Statistical significance was calculated using unpaired t-tests. *$p < 0.05$; **$p < 0.01$; ***$p < 0.001$; ****$p < 0.0001$; ns, not significant.

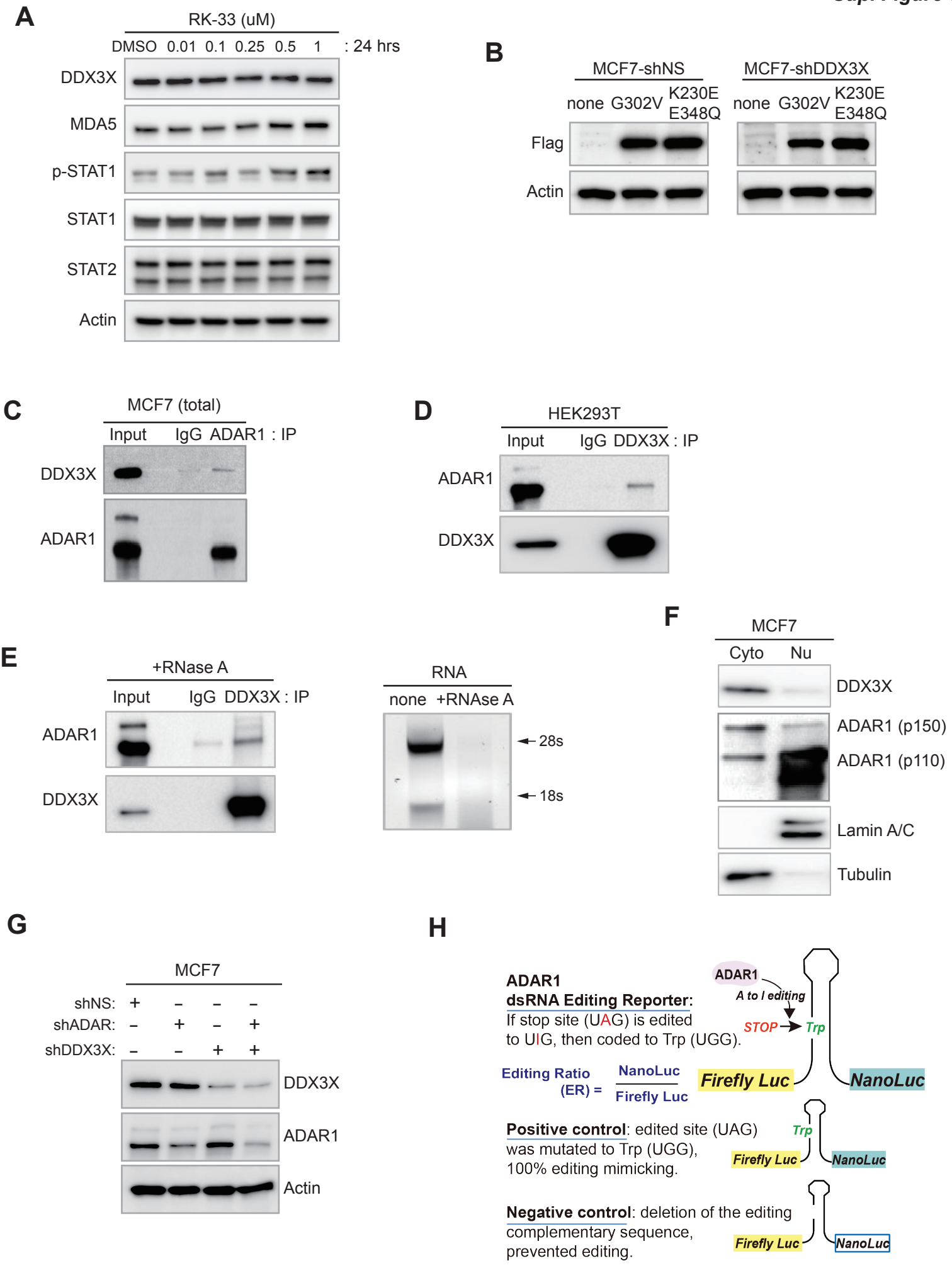
A
RK-33 (uM)
DMSO 0.01 0.1 0.25 0.5 1 : 24 hrs
DDX3X
MDA5
p-STAT1
STAT1
STAT2
Actin
B
MCF7-shNS
MCF7-shDDX3X
none G302V K230E E348Q
none G302V K230E E348Q
Flag
Actin
C
MCF7 (total)
Input IgG ADAR1 : IP
DDX3X
ADAR1
D
HEK293T
Input IgG DDX3X : IP
ADAR1
DDX3X
E
+RNase A
Input IgG DDX3X : IP
ADAR1
DDX3X
RNA
none +RNAse A
28s
18s
F
MCF7
Cyto Nu
DDX3X
ADAR1 (p150)
ADAR1 (p110)
Lamin A/C
Tubulin
G
MCF7
shNS: + – – –
shADAR: – + – +
shDDX3X: – – + +
DDX3X
ADAR1
Actin
H
ADAR1
dsRNA Editing Reporter:
If stop site (UAG) is edited
to UIG, then coded to Trp (UGG).
ADAR1
A to I editing
STOP
Trp
Editing Ratio (ER) = NanoLuc / Firefly Luc
Firefly Luc
NanoLuc
Positive control: edited site (UAG)
was mutated to Trp (UGG),
100% editing mimicking.
Trp
Firefly Luc
NanoLuc
Negative control: deletion of the editing
complementary sequence,
prevented editing.
Firefly Luc
NanoLuc

Supplementary Figure 6. DDX3X helicase activity is critical for regulating dsRNAs and DDX3X is associated with ADAR1-mediated A-to-I dsRNA editing.

A. Western blot analysis of phospho-STAT1, STAT1, STAT2, and MDA5 in RK-33 treated MCF7 cells for 24 hours.

B. Western blot analysis of overexpression of DDX3X mutants (G302V and K230E/E348Q).

C. Interaction between DDX3X and ADAR1 in MCF7 cells. IP was performed with ADAR1 antibody or control IgG.

D. Interaction between DDX3X and ADAR1 in HEK293T cells. IP was performed with DDX3X antibody or control IgG.

E. IP was performed with DDX3X antibody or control IgG and treated with RNase A (left). RNase A activity was confirmed by running RNA on the agarose gel (right).

F. Western blot of ADAR1 and DDX3X in cytoplasmic and nuclear fraction of MCF7 cells (Lamin A/C: nuclear marker, Tubulin: cytoplasmic marker).

G. Western blot validation of single or double knockdown of DDX3X and ADAR1 in MCF7 cells.

H. Schema of A-to I editing assay using dual luciferase assay system with positive and negative control vectors.

Data are representative of three independent experiments.

A

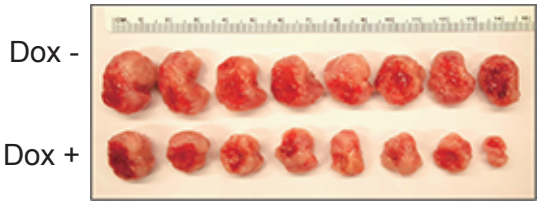
Dox -
Dox +

B

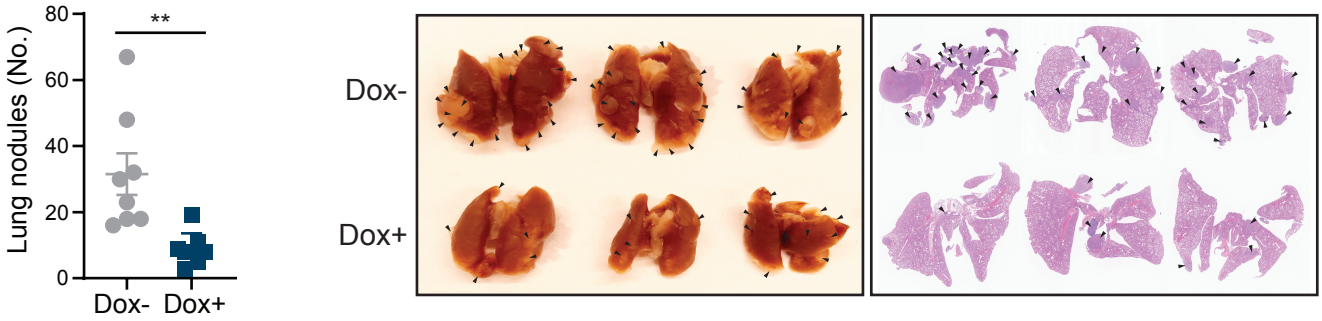
Lung nodules (No.)
80
60
40
20
0
**
Dox-
Dox+
Dox-
Dox+

C

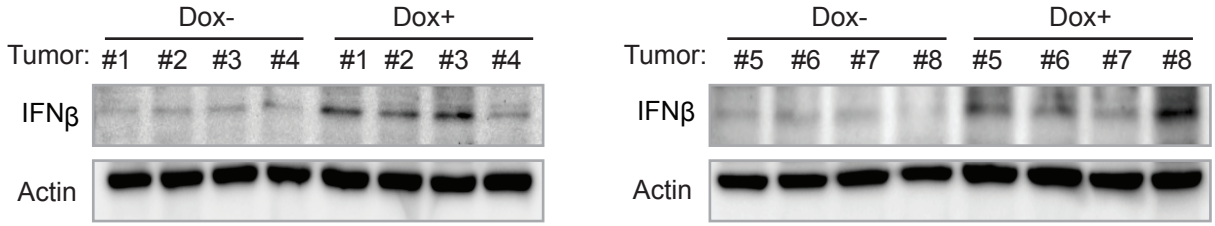
Dox-
Dox+
Tumor: #1 #2 #3 #4 #1 #2 #3 #4
IFNβ
Actin
Dox-
Dox+
Tumor: #5 #6 #7 #8 #5 #6 #7 #8
IFNβ
Actin

D

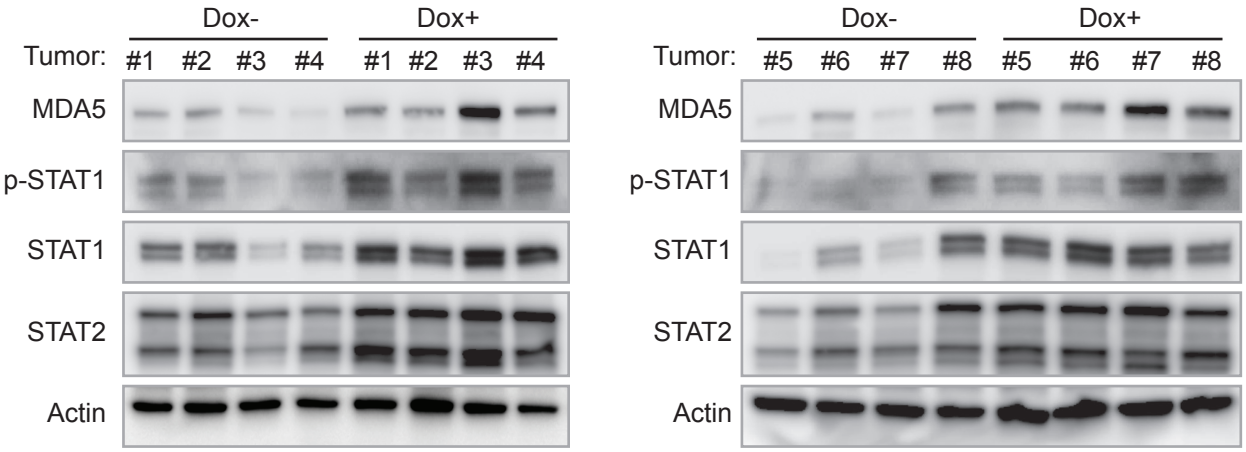
Dox-
Dox+
Tumor: #1 #2 #3 #4 #1 #2 #3 #4
MDA5
p-STAT1
STAT1
STAT2
Actin
Dox-
Dox+
Tumor: #5 #6 #7 #8 #5 #6 #7 #8
MDA5
p-STAT1
STAT1
STAT2
Actin

Supplementary Figure 7. Loss of DDX3X augments dsRNA sensing and IFN signaling in a syngeneic breast cancer model.

A. Images of tumors isolated from mice bearing 4T1 breast tumor with DDX3X-control (Dox-) or -inducible KD (Dox+).

B. Number of metastatic tumor nodules in lung (left) and representative lung images (right) of mice bearing DDX3X-control or -inducible KD 4T1 tumors.

C. Western blot of IFN-β in DDX3X-control (Dox-) or -inducible KD (Dox+) 4T1 tumors.

D. Western blot analysis of MDA5, phospho-STAT1, STAT1, and STAT2 in DDX3X-control (Dox-) or -inducible KD (Dox+) 4T1 tumors.

Data are represented as mean ± SEM. Unpaired t-tests. $^{**}P < 0.01$.

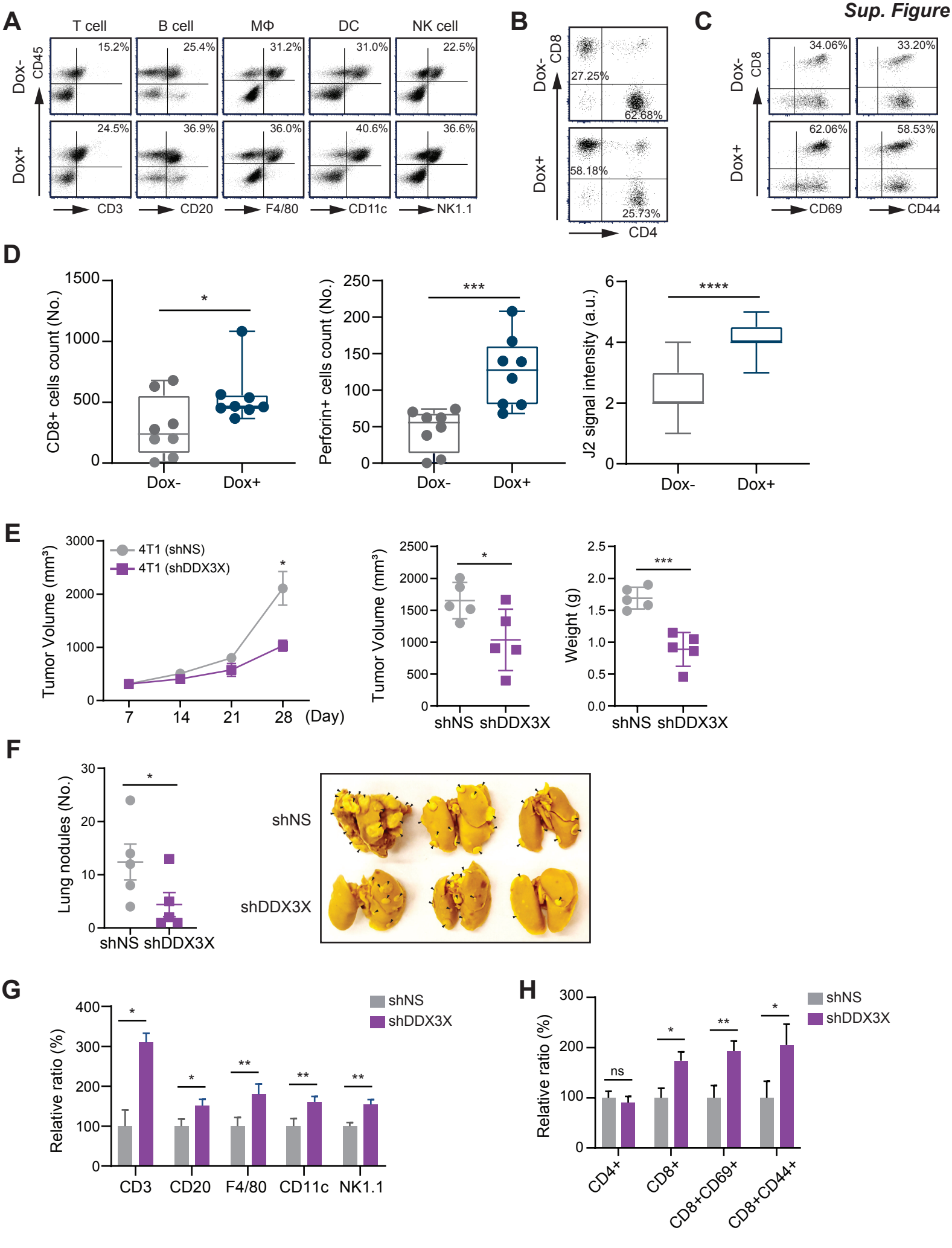
A
T cell
B cell
MΦ
DC
NK cell
Dox-
Dox+
CD45
15.2%
25.4%
31.2%
31.0%
22.5%
24.5%
36.9%
36.0%
40.6%
36.6%
CD3
CD20
F4/80
CD11c
NK1.1
B
Dox-
Dox+
CD8
27.25%
62.68%
58.18%
25.73%
CD4
C
Dox-
Dox+
CD8
34.06%
33.20%
62.06%
58.53%
CD69
CD44
D
CD8+ cells count (No.)
1500
1000
500
0
*
Dox-
Dox+
Perforin+ cells count (No.)
250
200
150
100
50
0
***
Dox-
Dox+
J2 signal intensity (a.u.)
6
4
2
0
****
Dox-
Dox+
E
Tumor Volume (mm³)
3000
2000
1000
0
4T1 (shNS)
4T1 (shDDX3X)
*
7
14
21
28
(Day)
Tumor Volume (mm³)
2500
2000
1500
1000
500
0
*
shNS
shDDX3X
Weight (g)
2.5
2.0
1.5
1.0
0.5
0.0
***
shNS
shDDX3X
F
Lung nodules (No.)
30
20
10
0
*
shNS
shDDX3X
shNS
shDDX3X
G
Relative ratio (%)
400
300
200
100
0
shNS
shDDX3X
*
*
**
**
**
CD3
CD20
F4/80
CD11c
NK1.1
H
Relative ratio (%)
300
200
100
0
shNS
shDDX3X
ns
*
**
*
CD4+
CD8+
CD8+CD69+
CD8+CD44+

Supplementary Figure 8. DDX3X-depleted tumor innate immunity is primed by dsRNA-stimulated tumor-intrinsic type I IFN.

A. Representative dot plots showing each cell marker expression of CD45+ cells isolated from DDX3X-control (Dox-) or -inducible KD (Dox+) 4T1 tumors. CD3+; T cell, CD20+; B cell, F4/80+; Macrophage, CD11c; dendritic cell, NK1.1; NK cell.

B. Representative dot plots showing CD4+ or CD8+ T cells isolated from DDX3X-control (Dox-) or -inducible KD (Dox+) 4T1 tumors.

C. Representative dot plots showing CD8+, CD69+, and CD44+ T cells isolated from DDX3X-control (Dox-) or -inducible KD (Dox+) 4T1 tumors.

D. Quantification of CD8, perforin positive cells, and J2 signal in IHC of Figure 7J.

E. Tumor growth (mm^3), volume (mm^3), and weight (g) in BALC/c mice bearing DDX3X-control or -stable KD 4T1 cells (5 mice/group).

F. Lung metastasis of DDX3X-control or -stable KD 4T1 tumors.

G. Quantification of each cell type after flow cytometric analysis of DDX3X-control or -stable KD 4T1 tumors. CD3+; T cell, CD20+; B cell, F4/80+; Macrophage, CD11c; dendritic cell, NK1.1; NK cell.

H. Quantification of each type of T cell after flow cytometric analysis of DDX3X-control or -stable KD 4T1 tumors.

Data are represented as mean ± SEM. Unpaired t-tests. **P* < 0.05; ***P* < 0.01; ****P* < 0.001; *****P* < 0.0001; ns, not significant.

Table S1. Primer list for qRT-PCR

Primer	Sequence (5'-3')
envV1 forward	GTGGCTCCATAACTTTGGAAAA
envV1 reverse	TAAGTGCAGCTGGTCCCAGTA
MER21C forward	GGAGCTTCCTGATTGGCAGA
MER21C reverse	ATGTAGGGTGGCAAGCACTG
MER57B1 forward	CCTCCTGAGCCAGAGTAGGT
MER57B1 reverse	ACCAGTCTGGCTGTTTCTGT
ERV-F(XA34) forward	CAGGAAACTAACTTTCAGCCAGA
ERV-F(XA34) reverse	TAAAGAGGGCATGGAGTAATTGA
ERV9-1 forward	TCTTGGAGTCCTCACTCAAACTC
ERV9-1 reverse	ACTGCTGCAACTACCCTTAAACA
MLTA10 forward	TCTCACAATCCTGGAGGCTG
MLTA10 reverse	GACCAAGAAGCAAGCCCTCA
Alu-1 forward	GTCAGGAGATCGAGACCATCCT
Alu-1 reverse	AGTGGCGCAATCTCGGC
Alu-2 forward	GAGGCTGAGGCAGGAGAATCG
Alu-2 reverse	GTCGCCCAGGCTGGAGTG
L1HS forward	AAAGCCGCTCAACTACATGG
L1HS reverse	TGCTTTGAATGCGTCCCAGAG

TaqMan Gene Expression Assay	
Primer	**Assay ID**
DDX3X	Hs00606179_m1
IFI44L	Hs00915292_m1
IFI44L	Mm00518988_m1
IFIT2	Hs01922738_s1
IFIT2	Mm00492606_m1
IFIT3	Hs00155468_m1
ISG15	Hs00192713_m1
STAT1	Hs01013996_m1
STAT1	Mm00439531_m1
STAT2	Mm00490880_m1
OAS1	Hs00973635_m1
OAS2	Hs00942643_m1
OAS2	Mm00460961_m1
MX1	Hs00895608_m1
TAP1	Hs00388675_m1
TAP2	Hs00241060_m1
PSMB8	Hs00188149_m1
HLA-A	Hs01058806_g1
HLA-B	Hs00818803_g1
HLA-C	Hs03044135_m1
HLA-DRA	Hs00219575_m1
DDX58 (RIG-I)	Hs01061436_m1
IFIH1 (MDA5)	Hs00223420_m1
IFIH1 (MDA5)	Mm00459183_m1
CCL5	Hs00982282_m1
IFNB1	Hs01077958_s1
IFNB1	Mm00439552_s1
18S	Hs99999901_s1

Primers for TASA-TD PCR	
Primer	**Sequence (5'-3')**
TAG-primer	GCACACGACGACAGACGACGCAC
Actb sense	GCTCGTCGTCGACAACGGCTCCGGCA
Actb antisense	CAAACATGATCTGGGTCATCTTCTC
Actb sense-tag	GCACACGACGACAGACGACGCACCAAACATGATCTGGGTCATCTTCTC
Actb antisense-tag	GCACACGACGACAGACGACGCACGCTCGTCGTCGACAACGGCTCCGGCA
Syncytin-1 sense	ATGGAGCCCAAGATGCAG
Syncytin-1 antisense	CTAACTGCTTCCTGCTGAATTGGGGCGTAG
Syncytin-1 sense-tag	GCACACGACGACAGACGACGCACCTAACTGCTTCCTGCTGAATTGGGGCGTAG
Syncytin-1 antisense-tag	GCACACGACGACAGACGACGCACATGGAGCCCAAGATGCAG
ERV9-1 sense	CTCTGGGGTCCTGACAACAT
ERV9-1 antisense	CCAGGTAGTCCCCACTACGA
ERV9-1 sense-tag	GCACACGACGACAGACGACGCACCCAGGTAGTCCCCACTACGA
ERV9-1 antisense-tag	GCACACGACGACAGACGACGCACCTCTGGGGTCCTGACAACAT

Table S2. Antibody Information

Western blot		
Antibodies	**Company**	**Catalog number**
rabbit anti-DDX3	Bethyl Laboratories	A300-474A
mouse anti-DDX3	Santa Cruz	sc-365768
rabbit anti-DDX1	Bethyl Laboratories	A300-521A
rabbit anti-DDX5	Bethyl Laboratories	A300-523A
rabbit anti-ADAR1	Bethyl Laboratories	A303-884A
rabbit anti-phospho-Stat1 (Tyr701)	Cell Signaling Technology	#9167
rabbit anti-Stat1	Cell Signaling Technology	#14994
rabbit anti-phospho-Stat2 (Tyr690)	Cell Signaling Technology	#4441
rabbit anti-Stat2	Cell Signaling Technology	#72604
rabbit anti-RIG-I	Cell Signaling Technology	#4200
rabbit anti-MDA-5	Cell Signaling Technology	#5321
rabbit anti-OAS1	Cell Signaling Technology	#14498
rabbit anti-Toll-like Receptor 3	Cell Signaling Technology	#6961
rabbit anti-phospho-PKR (Thr451)	Millipore	#07-886
mouse anti PKR	Santa Cruz	sc-6282
rabbit anti-phospho-eIF2α (Ser51)	Cell Signaling Technology	#9721
rabbit anti-eIF2α	Cell Signaling Technology	#9722
rabbit anti-cGAS	Cell Signaling Technology	#15102
rabbit anti-phospho-STING (Ser366)	Cell Signaling Technology	#85735
rabbit anti-STING	Cell Signaling Technology	#13647
rabbit anti-phospho-TBK1/NAK (Ser172)	Cell Signaling Technology	#5483
rabbit anti-TBK1/NAK	Cell Signaling Technology	#3504
rabbit anti-phospho-NF-kB p65 (Ser536)	Cell Signaling Technology	#3033
rabbit anti-NF-kB p65	Cell Signaling Technology	#8242
rabbit anti-phospho-IκBα (Ser32)	Cell Signaling Technology	#2859
mouse anti-IκBα	Cell Signaling Technology	#4814
rabbit anti-phospho-IRF-3 (Ser396)	Cell Signaling Technology	#29047
rabbit anti-IRF-3	Cell Signaling Technology	#11904
rabbit anti-phospho-IRF-7 (Ser477)	Cell Signaling Technology	#12390
rabbit anti-IRF-7	Cell Signaling Technology	#13014
rabbit anti-IFN-β1 (MouseSpecific)	Cell Signaling Technology	#97450
mouse anti-Lamin A/C	Santa Cruz	sc-376248
mouse anti-a-tubulin	Abcam	ab7291
mouse anti-FLAG M2	Sigma	F1804
mouse anti-β-Actin	Santa Cruz	sc-4777

Flow cytometry		
Antibodies	**Company**	**Catalog number**
Brilliant Violet 510 anti-mouse CD45 Antibody	BioLegend	103138
Brilliant Violet 605 anti-mouse CD3 Antibody	BioLegend	100237
PE/Cy7 anti-mouse CD20 Antibody	BioLegend	150420
PE/Dazzle 594 anti-mouse F4/80 Antibody	BioLegend	123146
Brilliant Violet 785 anti-mouse CD11c Antibody	BioLegend	117336
Brilliant Violet 711 anti-mouse NK-1.1 Antibody	BioLegend	108745
PE/Dazzle 594 anti-mouse CD4 Antibody	BioLegend	100456
Brilliant Violet 421 anti-mouse CD8a Antibody	BioLegend	100738
Brilliant Violet 785 anti-mouse CD69 Antibody	BioLegend	104543
PE/Cy7 anti-mouse CD44 Antibody	BioLegend	103030
APC conjugated anti-mouse H-2Kb bound to SIINFEKL	BioLegend	141605
APC conjugated anti-human HLA-ABC	BD Pharmingen	562006
APC conjugated anti-human HLA-DR	BioLegend	307609
J2 anti-dsRNA antibody	Scicons	10010500
APC conjugated mouse IgG2a isotype control	BioLegend	400219
APC conjugated mouse IgG1 Isotype control	BD Pharmingen	555751

Table S3. List of DEGs identified by RNA deep sequencing analysis related to Fig.1B

Differentially expressed genes (DEGs) and gene list from RNA deep sequencing in DDX3X-control and -knockdown MCF7 cells is available in the separate excel file. RNA sequencing data is available in GEO repository (accession number: GSE157323)

Supplementary Materials and Methods

Cell culture and Generation of stable cell lines

For generation of stable DDX3X knockdown cell lines, the following sequences were targeted: GIPZ Lentiviral Human DDX3X shRNA #1_Clone Id_V2LHS_228965: 5'-TAAATCTGACTCAAGATGG-3', GIPZ Lentiviral Human DDX3X shRNA #2_Clone Id_V3LHS_301003: 5'-GTACTGCCAACTCTCTCGT-3', GIPZ negative (non-targeting or non-silencing) shRNA control _Catalog ID_RHS4346, TRIPZ Inducible Lentiviral shRNA Human DDX3X #1_Clone Id_V3THS_301003: 5'-GTACTGCCAACTCTCTCGT-3', TRIPZ Inducible Lentiviral shRNA Human DDX3X #2_Clone Id_V2THS_228965: 5'-TAAATCTGACTCAAGATGG-3', SMART vector Inducible Mouse Ddx3x PGK-TurboRFP shRNA #1_Clone Id_ V3SM11253-232377132: 5'-TCCCTCTTGAATCACCCCG-3', SMARTvector Inducible Mouse Ddx3x PGK-TurboRFP shRNA #2_Clone Id_V3SM11253-232987995: 5'-TGCACTGCCAATTCTCTCG-3'. Recombinant lentiviral particles were produced using a protocol provided by the manufacturer (Addgene). In brief, 2 μg of shRNA-encoding vector DNA, 1.5 μg of psPAX2 (packaging vector) and pMD2.G (VSVG envelope vector) vectors were transfected into HEK293T cells in 94 mm^2 dish using the TransIT-LT1 Transfection Reagent (Mirus). Supernatants containing virus particles were collected 72 hours post-transfection. Filtered viral supernatants were added to the growth medium in the presence of polybrene (8 μg/ml). To establish stable KD cell lines, cells were selected 48 hours after viral infection using 2 μg/ml of puromycin and single colonies were isolated and propagated. Knockdown efficiency was validated by western blotting (protein) and qRT-PCR (mRNA). The

IFIH1, DDX58, and OAS1 genes were deleted respectively according to the manufacturer's instructions using a MDA5 (IFIH1) Human Gene Knockout Kit (OriGene, KN415661), RIG-I (DDX58) Human Gene Knockout Kit (OriGene, KN41615), and OAS1 Human Gene Knockout Kit (OriGene, KN400696), respectively.

Next-generation RNA-Sequencing and Data analysis

Total RNA was prepared from control and DDX3X knockdown MCF7 cells using TRIzol Reagent (15596026, Thermo Fisher) according to the manufacturer's protocol. RNA-seq libraries were prepared using the SOLiD Total RNA-Seq Kit (4452437, Applied Biosystem) and the library quality was checked using an Agilent 2100 Bioanalyzer. RNA sequencing was performed on an 5500XL SOLiD Sequencer (Applied Biosystem) according to the manufacturer's protocol. Reads were mapped to the human genome and genic read quantified using LifeScope Genomic Analysis Software and GRCh37 (hg19) genome and transcriptome annotations. Normalization, differential expression analysis, and principle component analysis were performed using R package DEseq2 version 1.45 (1). Heatmap was constructed using R package heatmap version 1.0.10. Differentially expressed genes (DEGs) were selected above FDR < 0.05 and fold change > 1.5. DEGs were used for input into Ingenuity Pathway Analysis (IPA). Gene Set Enrichment Analysis (GSEA) was performed using GSEA software with default setting and associated Molecular Signature Database (MSigDB) as previously described (2). GEO accession number: GSE157323

CCLE data analysis

Gene expression and gene effect data were obtained from the CCLE and DeMap portal (http://doi:10.6084/m9.figshare.11384241.v2). Cell lines from fibroblast and hematopoietic lineage were excluded from the expression profile analysis. DDX3X high expressing ($DDX3X^{hi}$) cells and DDX3X low expressing ($DDX3X^{low}$) cells were selected by DDX3X expression level (top 25% and bottom 25%, respectively). RNA-seq data, from selected groups, was normalized

using the voom method and differential expression determined by limma (3). MHC core scores were calculated with mean absolute deviation modified Z-score mRNA expression data in CCLE. The score was defined as the mean Z-score of all MHC class genes in each group. GSEA analysis was performed using fgsea function (4).

TASA-TD strand-specific PCR

Specific components from the SuperScriptIII First-Strand Synthesis System for RT-PCR (Life technologies) were used to perform reverse transcription with RNA from MCF7 cells. For the first strand cDNA synthesis reaction, 50 ng of RNA for β-*actin*, 400 ng for *Syncytin-1*, and 500 μg for *Env9-1* were used. 1 μM of a gene specific primer ligated to a TAG-sequence not specific for the human genome (GSP sense/antisense (RT) TAG) was implemented in the reaction. RNA and primers were preheated at 65°C for 5 minutes. The GSP-TAG, 0.5 mM dNTP, 5 mM $MgCl_2$, 10 mM DTT, 40 U RNaseOUT, 100 U SuperScriptIII RT, and 240 ng Actinomycin D (Sigma) were added to the RNA for a the total 20 μl reaction. Synthesis was performed at 50°C for 50 minutes and terminated at 85°C for 5 minutes. RT, with extremely low intrinsic RNase H activity (for cleavage of RNA from RNA/DNA duplexes), and Actinomycin D were added to prevent second strand cDNA RT resulting in antisense artifacts. After cDNA synthesis, 2 U of recombinant RNase H (Life Technologies) was added to each reaction and incubated for 20 minutes at 37°C. Afterward, gene and strand specific PCR was performed. PCR reactions were implemented with the EmeraldAmp GT PCR Master Mix (TAKARA) as described above (PCR analysis). To amplify sense and antisense cDNA, a TAG-primer and GSP sense (PCR) or a TAG-primer and GSP antisense (PCR) were used, respectively. We performed sense and antisense specific PCR using both sense and antisense cDNA of β-*actin* as an internal negative control that was previously demonstrated to have no antisense transcript (5). All cDNA products

were electrophoresed on 1% agarose gels, and visualized using Gel Red (Biotium). Primer sequence information is available in Supplemental Table 1.

Cell colony formation

Equal numbers of cells were seeded into 6 well plates in triplicate. Cells were fixed with 3.7% formaldehyde in PBS and permeabilized with 100% methanol followed by staining with 1% crystal violet. After staining, cells were washed and dried completely. Crystal violet stained cells were quantified by Image J (NIH) or, solubilized and measured by absorbance (OD 590 nm)

Immunoprecipitation

Cells were lysed in immunoprecipitation buffer (1% NP-40, 50 mM Tris-HCl, 500 mM NaCl and 5 mM EDTA) containing protease inhibitor cocktails (87785, Thermo Fisher) on ice for 30 minutes. Cell lysates (800 μg) were incubated with 3 μg of antibodies or normal IgG at 4°C overnight with rotary agitation. For immunoprecipitation of DDX3X, anti-DDX3X (sc-365768, Santa Cruz) antibody was used. Protein G agarose beads (11243233001, Roche) were added to the lysates and incubated for an additional 4 hours at 4°C with rotary agitation. The IP Beads were washed in immunoprecipitation buffer three times for 10 minutes each, to completely remove residual buffer, and boiled in SDS loading buffer for 10 minutes at 95°C for western blot analysis. For J2 immunoprecipitation, cells were fixed with 1 % formaldehyde prior to lysis of cells. Immunoprecipitation was performed with J2 antibody (10010200, Scicons) or normal IgG coupled to the protein G agarose beads.

Cytoplasmic and nuclear extractions

Cytoplasmic and nuclear fractionations were performed, according to manufacturer's instructions (78833, Thermo Scientific).

Flow cytometry

For tumor infiltrating leukocyte flow cytometry, tumors (0.5 g) were mechanically disrupted by chopping and then chemically digested using the Tumor Dissociation Kit (130-096-730, Miltenyi Biotec) and gentleMACS Dissociator (130-096-427, Miltenyi Biotec) according to manufacturer's instructions. Red blood cells were removed (10-548E, Lonza) from tumors and Fc receptors were blocked with anti-CD16/32 (101319, BioLegend) for 20 minutes on ice and then stained with appropriate antibodies for 1 hour on ice. Before flow cytometry analysis, cells were stained using the Zombie NIR Fixable Viability Kit (423105, BioLegend) to distinguish between live and dead cells. For OVA or HLA class expression on the cell surface, cells were detached with 2 mM EDTA in PBS and then washed twice using PBS before staining. Cells were stained with appropriate antibodies for 30 minutes on ice and then washed twice before flow cytometry analysis. Antibody information is provided in Supplemental Table 2. For J2 flow cytometry, cells were detached with 2 mM EDTA in PBS and then washed twice using PBS. Cells were fixed with 1x fixation buffer (424401, BioLegend) for 20 minutes at room temperature. After washing, cells were permeabilized with 0.1% Triton-X-100 in PBS for 15 minutes followed by incubation in 1% BSA in PBS for 30 minutes. Cells were stained with J2 antibody (10010200, Scicons) or mouse IgG2a isotype control (401501, BioLegend) for 1 hour at room temperature followed by anti-mouse IgG2 conjugated with APC secondary antibody.

Supplementary References

1. Love MI, Huber W, Anders S. Moderated estimation of fold change and dispersion for RNA-seq data with DESeq2. Genome Biol **2014**;15:550
2. Subramanian A, Tamayo P, Mootha VK, Mukherjee S, Ebert BL, Gillette MA*, et al.* Gene set enrichment analysis: a knowledge-based approach for interpreting genome-wide expression profiles. Proc Natl Acad Sci U S A **2005**;102:15545-50

3. Ritchie ME, Phipson B, Wu D, Hu Y, Law CW, Shi W*, et al.* limma powers differential expression analyses for RNA-sequencing and microarray studies. Nucleic Acids Res **2015**;43:e47
4. Sergushichev AA. An algorithm for fast preranked gene set enrichment analysis using cumulative statistic calculation. bioRxiv **2016**:060012
5. Chen J, Sun M, Kent WJ, Huang X, Xie H, Wang W*, et al.* Over 20% of human transcripts might form sense-antisense pairs. Nucleic Acids Res **2004**;32:4812-20